NSLS-II Beamline Development Proposal

Type I [x] Type II [ ]

Single-Crystal Spectroscopy & Macromolecular Crystallography at a 3PW Beamline (SM3)		
Allen M. Orville (Spokesperson)	Biophysicist BNL, Biology Department, Upton NY 11973	631-347-4739 amorv@bnl.gov
Deborah Stoner-Ma	Biophysicist BNL, Biology Department, Upton NY 11973	631- 344-6388 dstonerma@bnl.gov
Wayne A. Hendrickson	HHMI Investigator, University Professor Columbia University, New York, NY 10032	212-305-3456 wayne@convex.hhmi.columbia.edu
Marc Allaire	Biophysicist National Synchrotron Light Source, Upton NY 11973	631-344-4795 allaire@bnl.gov
Lonny E. Berman	Physicist National Synchrotron Light Source, Upton NY 11973	631-344-5333, berman@bnl.gov
Lisa M. Miller	Biophysicist National Synchrotron Light Source; Upton NY 11973	631-344-209 lmiller@bnl.gov
Annie Héroux	Biophysicist BNL Biology Department, Upton NY 11973	631-344-4454 heroux@bnl.gov
Howard H. Robinson	Biophysicist BNL Biology Department, Upton NY 11973	631-344-4789 hhr@bnl.gov
Dieter K. Schneider	Biophysicist BNL, Biology Department, Upton NY 11973	631-344-3423 schneider@bnl.gov
Alexei S. Soares	Biophysicist BNL Biology Department, Upton NY 11973	631-344-7306 soares@bnl.gov
Robert M. Sweet	Biophysicist BNL, Biology Department, Upton NY 11973	631-344-3401 sweet@bnl.gov
Wuxian Shi	Scientist, Case Western Reserve University at BNL, Upton NY 11973	631-344-2099 wushi@bnl.gov
Michael R. Sullivan	Engineer, Case Western Reserve University at BNL, Upton NY 11973	(631)344-3800 msullivan@bnl.gov

A. Science Case

Understanding the complex relationships among atomic structure, electronic structure, vibrational states, chemistry and catalysis is critical for obtaining fundamental insights into biological processes. Such processes include those that underlie human diseases or might inspire new catalysts for renewable clean energy sources. Consequently, new breakthroughs will come from a multi-disciplinary approach that includes several techniques to probe the structure and function of macromolecules. We will develop new tools at the NSLS-II to use several complementary techniques on the same sample, and under nearly identical experimental conditions. **In particular, we will build an integrated experimental station at the NSLS-II to support the nearly simultaneous, correlated measurements of these data:**

- ***i)*** **Macromolecular crystallography to high resolution**
- ***ii)*** **Electronic absorption spectroscopy**
- ***iii)*** **Steady-state and time-resolved fluorescence spectroscopy**
- ***iv)*** **Vibration spectroscopy (Raman and IR spectroscopy (from an adjacent IR beamline)**
- ***v)*** **X-ray absorption, extended x-ray absorption fine structure spectroscopy (XAS/EXAFS)**

With this suite of complementary methods, all fully integrated into the beamline-control environment, we will have created a unique facility. We will be able to correlate crystal structures with electronic structures and vibration states from the same sample – whether derived from resting-state(s) or trapped reaction intermediates – and under the nearly identical experimental conditions. Because we believe that correlated, complementary results are more significant than results obtained by individual techniques, the philosophy of the SMX & SM3 beamline teams is to support single-crystal spectroscopy and x-ray diffraction on a full-time basis. **The SM3 beamline will provide immediate continuity of the existing NSLS MX+Spec program at X26-C.**

The straightforward logic for our integrated facility at the NSLS-II allows us to build a flexible, modular system. A schematic of the concept at the sample is shown in Figure 1. The essential elements include:

I. Monochromatic x-ray photons in the ~5 – 25 keV energy range taken from a three-pole wiggler source (3PW)
II. A goniometer for three-axis rotation of a crystal about a eucentric point
III. A cryostream to control the temperature of the crystal (typically 100K with N_2, but also higher or lower with He cryostats)
IV. Up to four objective lenses, each aligned and focused at the rotation-point of the crystal, which also intersects the x-ray path
V. Spectroscopy light sources selected to deliver polychromatic photons or a particular excitation energy. These will include class 3B lasers and occasional use photons from an adjacent IR beamline
VI. Optical fibers to deliver and/or receive spectroscopic photons to/from the crystal
VII. Spectrometers to measure the absorption, Raman shift, or fluorescence emission spectrum

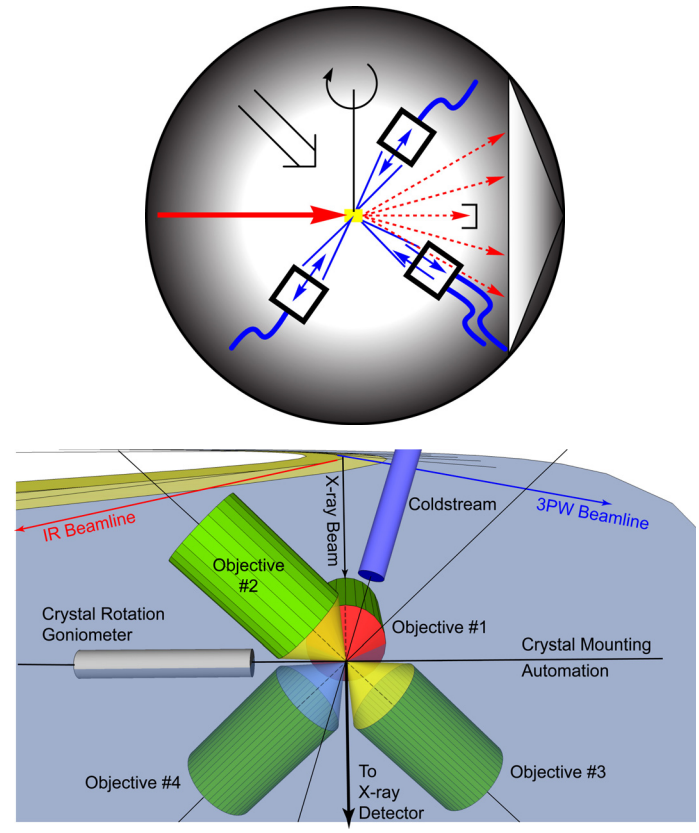

Fig. 1: *A conceptual layout for collecting single-crystal spectroscopic and x-ray diffraction data from cryo-cooled crystals at the SM3 and SMX beamlines.*

Background - Macromolecular crystallography (MX) is the preeminent method for structural biology world-wide. It often garners Nobel Prize attention with seven awards in the past 13 years. The frontier challenges for MX include structures of trapped reactive intermediates, large macromolecules and viruses, membrane proteins, protein-protein complexes, and protein-nucleic acid complexes (*1*). Approximately one-third of all macromolecules expressed by all organisms contain an essential cofactor (*2*). Those cofactors with color, such as metal ions and/or organic molecules, are present in roughly 11,000 entries in the PDB archive (see Table 1). These macromolecules usually exhibit a characteristic spectroscopic signature that changes during catalysis. Indeed, all biological macromolecules of relevance to energy and photosynthetic systems, separate charge and transfer electrons using proteins that contain cofactors and/or post-translational modifications. Cofactors and chromophores are also involved in metal transport and homeostasis, light sensing systems, the entire green fluorescent protein superfamily, nitric oxide synthesis and signaling, redox-state and stress-response systems, and managing the toxicity of reactive oxygen and nitrogen species. Cofactors are also present in RNA and other nucleic acid-based macromolecules, which often provide essential structural complexity, plasticity, and catalytic activity. **Therefore, our single-crystal spectroscopy facility will support interdisciplinary research that impacts nearly all of biology, from pathogenic and beneficial microbes to humans to the plant kingdom.**

Consider further that many cofactors are altered by solvated electrons and/or radical species generated by the interaction of the x-ray photons with the crystal and its contents. Consequently, unanticipated electron

Table 1: Summary of Selected Cofactors Within Structures Deposited in the PDB Archive (June, 2010)

Prototypical Protein Example	Cofactor or Chromophore	λ_{max} (nm)	Typical ε (mM^{-1} cm^{-1})	PDB Ligand ID or Name	No. PDB Structures
Aspartate Aminotransferase	Pyridoxal-5´-phosphate	350, 412	6.6, 9.5	PLP	568
Lactate Dehydrogenase	NAD(H) or NADP(H)	340	6.2	NAD, NDP, NAP	1480
Dihydrofolate Reductase	Pterin	350	4.5	Pterin	242
p-Hydroxybenzoate Hydroxylase	FAD or FMN	450	11	FAD, FMN, flavin	1466
Myoglobin	Heme	409	170	Hem	2262
Mn Superoxide Dismutase	Mn(III)-O/N	480	0.91	Mn	1395
Rubredoxin	Fe (non-heme)	430 - 500	3 - 5	Fe	766
Ferredoxin	Fe_2/S_2 Cluster	~400	30.6	FeS	304
High Potential Iron Protein	Fe_4/S_4 Cluster	~400	15	SF4	388
Methylmalonyl-CoA Mutase	Co or B_{12}	360	27.5	Cobalt	355
Urease	Ni(II)-O/N	407	0.21	Nickel	461
Azurin or Plastocyanin	Cu	600	5	Cu	752
Photosynthetic Reaction Center	Chlorophyll	465, 665	>100	BCL, BPH, etc	147
Bacteriorhodopsin	Retinal	480	27	Ret	111
Green Florescent Protein	Post-translation modification	350 - 700	6 - 138	Luminescent Proteins	218

density, or "observations" of color changes during x-ray diffraction studies are difficult to explain based upon the structure alone. Moreover, far less than 1% of the crystal structures identified by the analysis summarized in Table 1 were correlated with any type of single-crystal spectroscopy. This raises questions about the many important structures in the PDB. In contrast, single-crystal spectroscopy correlated with x-ray diffraction provides data to remove the mystery from the interpretation of such "mystery density". Without question, the best correlations of atomic and electronic structure derive from results that are obtained from the same crystalline samples, which ultimately yield the most profound mechanistic insights.

Heme-based enzymes have perhaps the oldest and richest history in protein crystallography, and exhibit a molar absorptivity that is among the highest for all protein cofactors (see Table 1). Indeed, research over the past 50 years into the structure and function of heme proteins has produced iconic, landmark results, including the 1962 Nobel Prize in Chemistry to Max F. Perutz and John C. Kendrew "for their studies of the structures of globular proteins." And yet, correlated crystallographic and spectroscopic studies are just now providing critical new insights into the nature of reactive intermediates along the reaction coordinate for only a few of these proteins. For example, high-valent intermediates for several heme-containing proteins have been generated and studied by correlated methods including: cytochrome *c* peroxidase Compound I, cytochrome $P450_{cam}$, chloroperoxidase, horseradish peroxidase, catalase, and the peroxidase activity of myoglobin. Moreover, the ability to distinguish between Fe(II)-OH_2, Fe(III)-OH, Fe(III)-O-O(H) and Fe(IV)=O species based on electron density maps is nearly impossible in the absence of sub-Ångström resolution data. In contrast, the vibration-sensitive and x-ray absorption spectroscopic features of these species are often dramatically different. Consequently, the use of correlated spectroscopic and crystallographic analysis is essential to assign chemical and mechanistic insight(s) to typical resolution structures (*3-6*).

An important example of how correlated studies at beamline X26-C were used to trap a reactive intermediate was published recently in *Biochemistry* (*7*) by Dr. Orville in collaboration with Drs. Gadda and Prabhakar. Figure 2 illustrates some of the key results. Choline oxidase (CHO) from *Arthrobacter globiformis* is a FAD-dependent enzyme that catalyzes the two-step, four-electron oxidation of choline to glycine betaine, with betaine aldehyde as a two-electron oxidized intermediate. In the two oxidative half-reactions, two molecules of

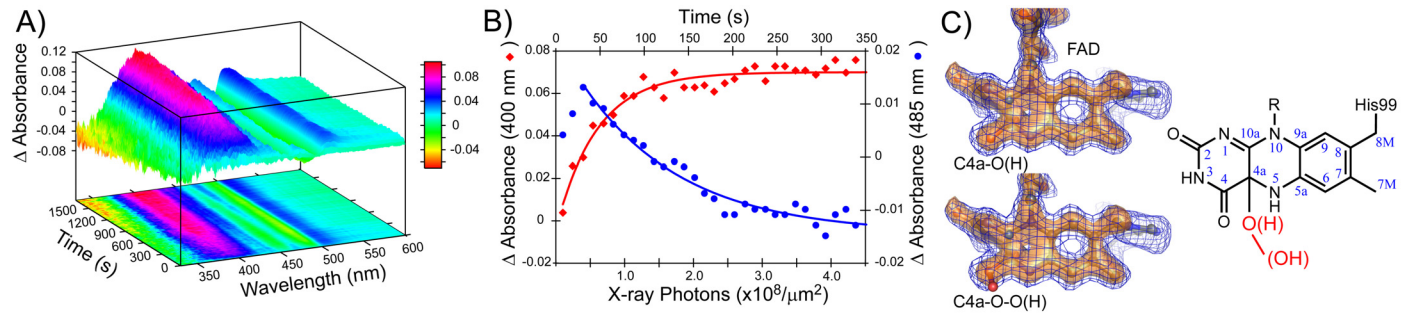

Figure 2: Evidence for the flavin C4a-oxygen adduct in choline oxidase; (A, B) time course for adduct generation in the x-ray beam, (C) the atomic structure of the adduct is consistent with either one or two oxygen atoms bound to C4a.

O_2 are converted into two H_2O_2 molecules. We performed several spectroscopic measurements on a number of choline oxidase crystals including before and after x-ray exposure. Importantly, the difference spectra (after – before) clearly shows a spectrum with λ_{max} at 400 nm that is nearly identical to spectra obtained from flavin C4a-OOH or C4a-OH enzyme reaction intermediates. Typically these reactive oxygen intermediates exhibit half-lives of only several milliseconds in solution, but remarkably, it is stable in the crystal at 100K. The time-dependent results show that this species is generated with a $t_{1/2}$ of approximately 40 seconds upon x-ray exposure. Moreover it is formed commensurate with the decrease of the 460 and 485 nm features attributed to oxidized FAD. The resulting electron density maps (unbiased simulated annealing at 1.8 Å resolution) and the interpretation of the atomic structure is consistent with two possible reactive oxygen species, namely a covalent flavin C4a-OOH and/or C4a-OH adducts. Either structure correlates well with the spectroscopic observations. Moreover, the complementary nature of the two types of data reinforces the conclusions; whereas either type of data alone yields somewhat ambiguous results.

SM3 in synergy with SMX – The SMX and SM3 beamlines, with their diverse and complementary end station components will provide unique capabilities for highly correlated single-crystal spectroscopy and x-ray diffraction. Ideally, the SMX and SM3 beamlines should be sited immediately adjacent to each other to facilitate coordinated operations, integration of various techniques, and to more easily share some of the spectroscopy components, especially those that utilize optical fibers. One specialty of SM3 that is not covered by SMX is single-crystal XAS/EXAFS/XANES. Similarly, one specialty of SMX that is not possible at SM3 is nuclear resonance vibration spectroscopy (NRVS).

SM3 in synergy with an IR Beamline – As outlined below, IR spectroscopy is complementary to Raman spectroscopy. Consequently, the location of the SMX and SM3 beamlines nearby an IR beamline will provide an opportunity to collect FTIR spectroscopic data from single-crystals. Indeed, the SM3 beamline and an IR beamline are likely to be the most closely located to each other.

SM3 in synergy with an off-line laser optics lab – As outlined below, we also propose to build an off-line laser-optics laboratory located downstream from the SM3 end station x-ray hutch. This will provide additional experimental conditions. On-line studies that take place inside the x-ray hutch require that nothing prevents diffracted x-rays from reaching the area detector. Because the off-line apparatus in the adjacent laser/optics laboratory requires no equipment-free zones, it has more direct-axis orientations that can exploited by spectroscopy components. This will facilitate characterization of samples prior to x-ray exposure and will accommodate samples from other beamlines at the NSLS. Moreover, the on-line and off-line facilities may share instrumentation and optical fiber connections and thus, they will complement each other.

SM3 in synergy with other MX Beamlines – The SM3 beamlines are part of the six macromolecular crystallography beamlines proposed for NSLS-II as envisioned by the greater MX community at the NSLS. Each of the MX beamlines will fill a unique niche, and as a group they will provide the best possible facilities for regional, national, and international scientists. However, a common feature to all MX beamlines will likely be the ability to collect electronic absorption spectroscopic data as a function of x-ray diffraction. The SMX and MX3 beamlines and staff will help this capability. It will also serve to identify those projects that will benefit

from more comprehensive studies at the SMX, SM3, or off-line laser spectroscopy lab. Here's the whole roster and a brief summary of each MX beamline:

FMX	Frontier micro-focusing MX at an undulator.	Tunable 1 to 100μm beams, preservation of coherence, diverse crystal-manipulation apparatus and automated specimen delivery.
AMX	Flexible access, highly automated MX at an undulator.	Tunable 5 to 300μm beams, crystal screening automation, convenient access for experimenters.
AM3	Flexible access MX at a 3PW.	Tunable 25 to 300μm beams, crystal screening automation, convenient access for experimenters.
SMX	Coordinated MX and single-crystal spectroscopy viewing a canted IVU20 undulator, low-β straight section.	~5 to 25keV; 10 to 300μm beam size; spectroscopies to include electronic absorption, fluorescence, Raman and IR; automation for crystal mounting and integrated data collection.
SM3	Coordinated MX and single-crystal spectroscopy at a 3PW.	~5 to 25keV; 25 to 300μm beam size, spectroscopies to include electronic absorption, fluorescence, Raman and IR, and XAS/EXAFS; full automation.
NYX	NYSBC Microdiffraction at an undulator	Novel high-energy-resolution monochromator produces 5-50μm beams, accurate goniometer, pixel-array detector.

B. Beamline Concept & Feasibility

We anticipate providing this capability to the general user community within the first days of NSLS-II operations to provide continuity to our current users. Our goal is to provide a beamline that supports the nearly simultaneous measurements of x-ray diffraction and several types of single-crystal spectroscopic data. To achieve this goal, we will reuse those NSLS components that are suitable for the SM3 beamline. The NSLS-II beamline transition working group has explored equipment reuse issues, which may be partially supported using "early operations funds". Ideally, SM3 will be located adjacent to the SMX beamline, the undulator-based compliment to support simultaneous single-crystal spectroscopy with macromolecular crystallography. We will draw upon our experience with integrating single-crystal spectroscopy and x-ray diffraction at beamline X26-C of the NSLS. This includes recent support from the DOE-BER and the NIH-NCRR to accelerate building the on-line and off-line stations for single-crystal spectroscopy at NSLS beamline X26-C.

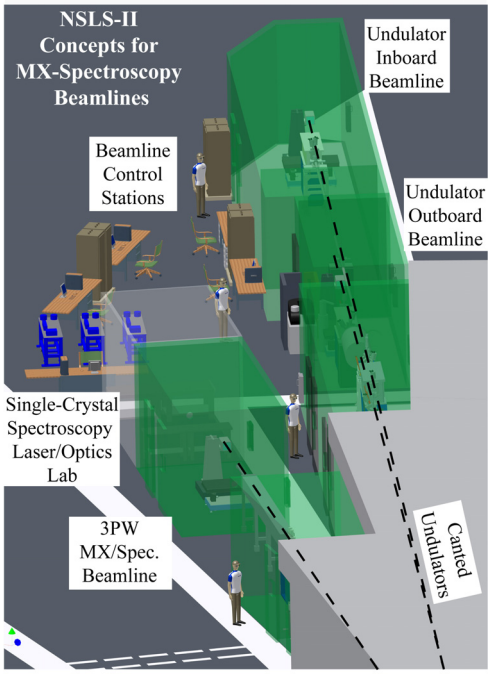

Fig. 3: *A conceptual layout of SM3 adjacent to canted undulater-based MX beamlines.*

Macromolecular Crystallography –

The *NSLS-II Conceptual Design Report* and our preliminary studies provide a conceptual design of tunable MX beamline that will be well-suited for correlated single-crystal spectroscopy and x-ray diffraction (Fig. 3). The SM3 beamline will use x-ray photons in the 5 – 25 keV range from a 3PW source. The x-ray optics will be optimized to deliver an adjustable x-ray beam size in the range of ~25 – 300 μm. This will match the spectroscopy spot sizes in the near UV to IR wavelength range that are delivered by various microscopic objective lenses. Motorized crystal motions will provide submicron-accuracy positioning and eucentric rotation about at least two axes. Sample cryogenics and remote crystal automounters will be deployed. It is likely that a high performance CCD-based large-format area detector will be available from either NSLS beamline X25, X29 (ADSC Q315R) or X6A (ADSC Q270), or possibly a Pilatus-like detector.

X-ray Source and Optics: The x-ray beam source at the 3PW will be ~167 μm x ~12 μm (σ_h x σ_v). We should realize a brightness of

about 5 x 10^{15} ph/s/.1%bw/mm^2/$mrad^2$ at the energies typically used for anomalous phasing, and an estimated flux of about ~10^{12} ph/s at 12 keV. The horizontal divergence in the beam will be up to 2 mrad and controlled with apertures, which will decrease the x-ray flux. The vertical divergence will be about 0.2 mrad. To monochromatize the white beam radiation, we propose to use components from either X25 or X29. These beamlines use cooled double crystal Si111 monochrometers with a horizontal focusing, sagittal bend at the second mono crystal. It typically produces magnification ratios between 1:1 and 4:1. Both X25 and X29 deploy a second vertically focusing mirror downstream from the monochromator. At SM3 we could either reuse the X26-C or X25 focusing mirrors. Together these components will provide a ~25 – 300 µm range of beam sizes.

Several other design possibilities are still under evaluation. For example, improvements might be realized by using as much of the 3PW emission fan as possible, placing a toroidal focusing mirror or a collimating mirror in the front end, and/or focusing to a secondary source prior to the monochromator. Regardless of the final design, we anticipate installing beam diagnostic devices along the x-ray path to support real-time auto-alignment methods. To that end, we will place beam position monitors and/or high-resolution beam profile imaging devices before and/or after each major optical element to provide feedback to the alignment control devices.

Single-Crystal Spectroscopy –

a) UV/Vis electronic absorption – We further illustrate the concept of nearly simultaneous single-crystal spectroscopy and x-ray diffraction with our setup at beamline X26-C (Fig. 4). It consists of a Crystal Logic diffractometer with an ADSC Q210R area detector, a 4DX-ray Systems AB optical system, a Newport 75W Xe research arc lamp (~350 - 850 nm), and an Ocean Optics USB 4000 CCD-based spectrophotometer operated through EPICS within a LINUX operating system. The 15x Schwarzschild parabolic mirror microscope objectives are free from chromatic aberration. The incident light passes through a 50 µm optical fiber and is focused by objective #1 to 25 µm diameter spot. Transmitted light is collected from a 75 µm diameter region focused by objective #2 and connected to a 400 µm optical fiber. Each spectrum typically takes about 100 milliseconds to collect. We integrated the diffraction and spectroscopy techniques into the beamline control software, which coordinates data collection and links the results to our PXdb tracking database. Before and after x-ray diffraction, anisotropic single-crystal electronic absorption spectra are collected as a function of crystal rotation angle. During x-ray diffraction, an absorption spectrum is collected from the crystal at its "best" angle during the x-ray detector readout time after each frame of diffraction data. Anticipated improvements at the NSLS-II will include new Schwarzschild type mirror objectives with at least a 35 mm working distance. These new objectives will also include slots to allow for inserting various band-pass and/or polarizing filters. The longer working distances will provide sufficient space for two rotation axes of the crystal (kappa and omega).

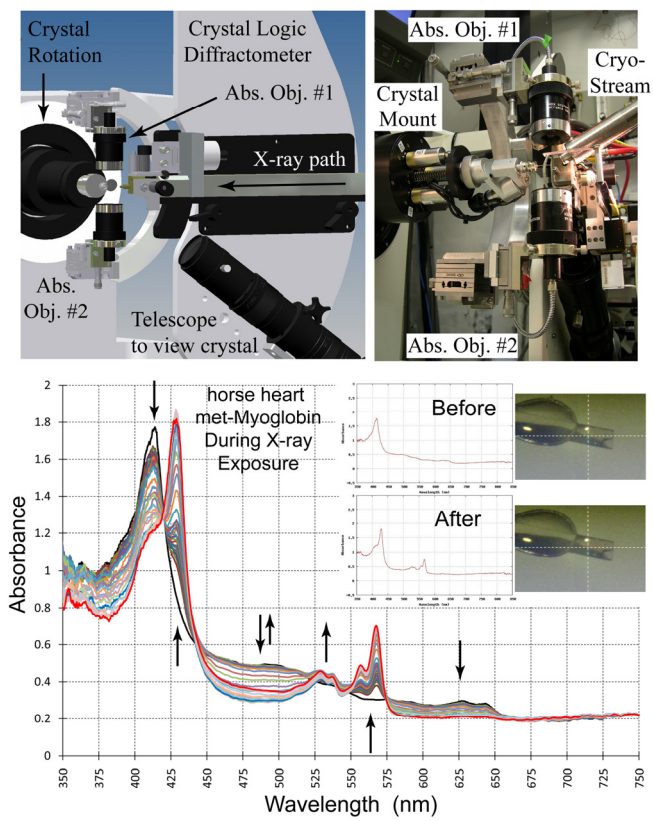

Fig. 4: The spectroscopy + MX setup at beamline X26-C (top), and an example of correlated single-crystal spectroscopy with x-ray diffraction collected from met-myoglobin (bottom).

b) Steady-state and time-resolved fluorescence – Steady-state and time-resolved fluorescence spectroscopy are extremely sensitive techniques with applications relevant to most molecules throughout biology. For example, NAD(P)H, flavins, pyridoxal 5'-phosphate, nucleic acids, tryptophan, 2-aminopurine,

and nitrotyrosine all yield strong fluorescence spectra. We will deploy apparatus for fluorescence spectroscopy at both the on-line and off-line spectroscopy stations. Ocean Optics QE65000 scientific-grade spectrometers preconfigured for fluorescence spectroscopy will measure data from steady-state fluorescence-emission and time-correlated single-photon-counting (TCSPC) studies (*8*). These will be controlled under EPICS and integrated into the x-ray diffraction and other spectroscopy methods. Several class 3B lasers for fluorescence-excitation will be coupled to optical fibers to deliver excitation photons to the sample.

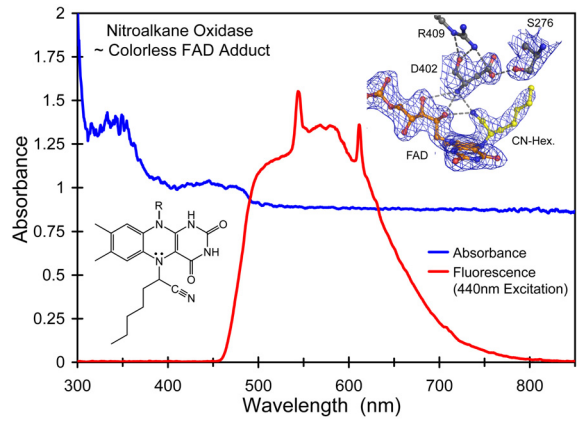

Fig. 5: *Low temperature crystals of the trapped adduct in nitroalkane oxidase yield consistent information from electronic absorption and fluorescence spectroscopy, as well as x-ray crystallography and chemical information.*

AMO has collected steady-state fluorescence spectroscopic data at the CryoBench facility at the ESRF. For example, nitroalkane oxidase catalyzes the oxidation of neutral nitroalkanes to nitrite and the corresponding aldehydes or ketones. The oxidative half-reaction is completed with conversion of O_2 to H_2O_2. The optical properties of the wild-type enzyme include a λ_{max} near 450 nm, which results from the oxidized FAD. When the enzyme oxidizes nitroalkanes in the presence of cyanide, an electrophilic flavin imine intermediate can be trapped (Fig. 5) (*9*). This trapped intermediate is almost colorless because the FAD isoalloxazine ring is formally reduced. We co-crystallized the trapped adduct for correlated studies at beamline X26-C and the CryoBench at the ESRF. The optical absorption spectrum, fluorescence spectrum, chemical formula, and electron density maps for the FAD N5-cyanohexyl adduct are shown in Figure 5. The optical spectrum from these crystals at low temperature shows very little absorbance in the visible region, but does exhibit a larger feature at approximately 340 nm. This is consistent with electronic absorption spectra collected from the same complex trapped in solution. The fluorescence-emission spectrum with 440 nm excitation is also consistent with studies of enzymes in solution, with additional features that likely arise from the crystal morphology (*9, 10*). Finally, the x-ray crystal structure of the colorless complex shows the N5 covalent adduct. Thus, the correlated spectroscopic data and x-ray diffraction provided important information about this trapped intermediate, and by extension to the proposed reaction mechanism for the enzyme.

c) Resonance and near-IR Raman – Structure and function are undeniably linked. Since the Raman effect involves interactions between atomic positions, electron distribution, and intermolecular forces, it is ideally suited to provide insights into function that a crystal structure alone cannot. Indeed, the information available from Raman spectroscopy can be very detailed, exceeding the level of resolution found in all but the highest resolution x-ray crystal structures. It can also reveal changes in the distribution of electrons in a bound ligand as well as details about hydrogen bonding strengths between active site residues and substrate or inhibitor molecules.

Despite these characteristics, Raman spectroscopy has not been widely exploited in biochemistry because of three inherent difficulties: a) low Raman sensitivity, b) interference from fluorescence background, and c) difficult data interpretation. The latter problem becomes readily apparent when one considers that the number of vibrational modes present in a molecule is $3n - 6$, where n is the number of atoms; this is quite large for macromolecules. Therefore, the complete Raman spectrum of a macromolecule is very complex; it probes vibration bands inherent to all the chemical bonds throughout the macromolecule. Consequently to be most effective, Raman spectroscopy is often applied to systems where one can focus upon a small region of interest, such as an enzyme active site, or by recording the Raman difference spectrum as a function of ligand binding or crystal orientation. Isotopic editing – wherein the ligand of interest is selectively or uniformly labeled with stable isotopes such as ^{2}H, ^{13}C, ^{15}N, ^{17}O, ^{18}O, ^{19}F, ^{34}S, ^{57}Fe *etc.* – is also a powerful method to identify the Raman bands of interest since they shift to a lower frequency with the isotopic substitution. Another effective strategy is to use resonance Raman, which requires laser excitation within an allowed electronic transition.

Because resonance Raman increases both the sensitivity and the selectivity of the technique, it has been successfully applied to macromolecules containing colored cofactors. Finally, resonance Raman coupled with isotopic editing is a powerful method to define otherwise very complex systems. Not surprisingly then, Raman spectroscopy is experiencing a renaissance, especially in applications where it is coupled to microscope optics, and consequently probes small volumes and/or single crystals.

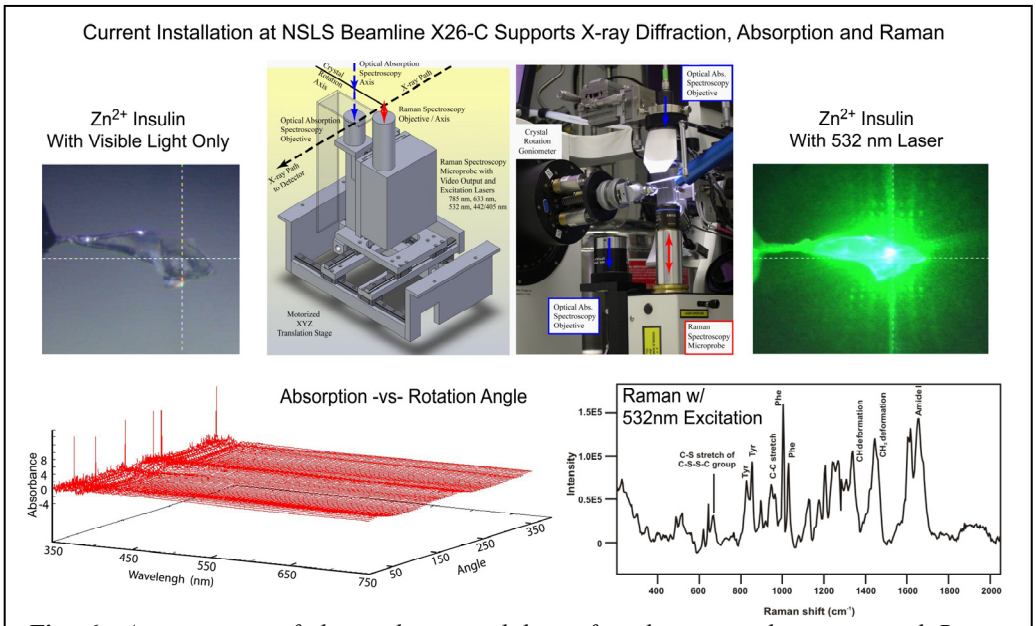

Fig. 6: *An overview of the on-line capabilities for electronic absorption and Raman spectroscopy at NSLS beamline X26-C.*

We are currently commissioning a Raman microspectroscopy system (Fig. 6) with two excitation wavelengths (785 nm and 532 nm) with two additional excitation sources (e.g. 633 nm, and 473/442/405 nm) soon to be added. The objective lens of the Raman microprobe focuses the laser onto, and collects scattered photons from, the sample. Such coaxial backscattering geometry ensures identical Raman excitation and detection volumes from the same ~25µm diameter region of the crystal that intersects the x-ray beam and the electronic absorption optics. A video interface inside the microprobe head facilitates alignment of the laser to the crystal. Motorized XYZ kinematic translation slides will provide accurate alignment of the laser focal spot to the crystal and the x-ray beam. Because the system uses high-grade quartz optical fibers, the Raman system is compatible with studies conducted on-line (inside the x-ray hutch) or off-line (in the adjacent laser/optics lab). We will control the instrumentation with external triggers over our local area network and it with our Linux-based data acquisition control software. This will enable us to synchronize the x-ray diffraction, optical absorption, and Raman scattering experiments. As shown in Figure 6 (lower left), the absorption spectra of Zn^{2+} insulin crystals as a function of rotation angle is essentially spectroscopically "silent." In contrast excitation with the 532nm Raman laser yields rich Raman stretching features from within the protein molecules of the crystal (lower right). This includes aromatic residues and information related to the disulfide bond, the latter of which is susceptible to degradation by x-ray dose.

d) IR Spectroscopy – We will develop single-crystal FTIR spectroscopy to complement the other optical methods outlined above. For example, IR and Raman vibration spectroscopies naturally complement each other. Their selection rules differ and are functions of the molecular polarizability between the electrons and nuclei within the molecules. Thus, molecules that elicit strong IR bands may only yield very weak Raman signals and *vice versa*. As an example, some metalloenzymes of relevance to H_2 and C_1 catalysis utilize metal coordination spheres that yield strong IR signatures, but weak Raman bands. We envision that on a part-time basis, the IR spectroscopy photons will come from an adjacent IR beamline within the Bio-Village at the NSLS-II. The high brightness and polarization of the synchrotron infrared source will provide high S/N spectra from small, oriented single crystals. This requires the cooperation and integration of two adjacent beamlines and will yield a unique capability.

e) Single-crystal XAS / EXAFS / XANES spectroscopy – X-ray absorption spectroscopy (XAS), which includes extended X-ray absorption fine structure (EXAFS) and X-ray absorption near edge spectroscopy (XANES) provides atomic-level information primarily focused on the transition metal K absorption edges (6 -

12 keV). Indeed, the metrics available from this type of analysis are much more accurate than the typical resolution crystal structure. Thus, the information content is particularly complimentary to x-ray diffraction and has applications especially in the structural and spectroscopic analysis of metalloenzymes and high-valent reactive intermediates. However, there is also a need for higher energy K edges of heavy elements such as Cd, Se, Pd, Ag, Mo, W, and Sb, which also offers improved sample penetration. This will be valuable for metalloenzymes isolated from microbes that inhabit extreme-environments such as the deep-sea hydrothermal volcanic vents. In addition, lower energy XAS shows great potential for biologically-important lighter elements (Ca, S, P, Mg), advantageous use of heavier element L and M absorption edges, and also combined studies of redox reactions. x-ray diffraction and XAS from the same crystalline sample has be achieved elsewhere (*11-15*), but always on a part-time basis, which often frustrates researchers dependent upon highly correlated studies (*e.g.* see C. Wilmot letter of support in Appendix III). Thus, the addition of XAS along with x-ray diffraction and vibration-sensitive techniques at the SM3 beamline will provide a novel and complementary capability to the SM3 beamline.

XAS data are measured in fluorescence mode and usually approximately at a right angle to the x-ray path. Often the detector exploits a 30-element or more solid-state Ge detector. The detector, with its auxiliary cooling and electronics, can occupy a relatively large footprint near the sample. Under some circumstances this will conflict with other instruments, such as the x-ray diffraction area detector, especially under high resolution conditions (short crystal – detector distance). Consequently, one possibility is to mount the Ge detector on a motorized slide for remote positioning relative to the sample. This will allow one to optimize both the count-rate levels for XAS data and the x-ray diffraction detector for crystallographic data.

f) A complementary off-line single-crystal spectroscopy laboratory – An essential element of our overall plan is the off-line single-crystal spectroscopy facility. It will include all the optical and vibrational spectroscopic analysis as the on-line systems. However, because the off-line lab does not impact x-ray beamtime, nor require unencumbered downstream cones for x-ray diffraction, it will also permit more sophisticated studies that require additional spectroscopic objectives. We plan to locate the laser/optics lab immediately adjacent to the 3PW and undulator beamlines as illustrated in Fig. 2 above. Optical fibers will connect the off- and on-line stations.

Anticipated Unique Capabilities: The technologies we envision for the NSLS-II will be unique in the United States and potentially throughout the world. The scientific problems that we and our users will address are central to the progress of macromolecular sciences in the United States. The national resource we envision will support unprecedented, highly correlated studies. The results will provide much needed data on the complex relationships among macromolecular atomic structure, electronic structure and chemistry. These data will be used by the large number of national and international researchers in the field. Realization of our plans for NSLS-II will place the United States in a leadership position in this area.

Our integration of complementary methods applied to macromolecular crystals at X26-C currently leads the world. Single-crystal spectroscopy provides powerful experimental data to help identify the chemical and electronic composition of otherwise ambiguous atomic features observed in crystallographic electron density maps. Correlated multidisciplinary studies on the same crystalline sample, under the same experimental conditions, facilitate the complete extraction of potential data from each sample. It is also important to note that x-ray and/or laser irradiation often promotes photochemistry, even at cryogenic temperatures. This will be of value for many systems of relevance to NIH and DOE missions. Moreover, our multidisciplinary research philosophy provides a novel intellectual and highly collaborative environment that will benefit many projects.

C. Required Technical Advances

One particular feature of our anticipated Raman setup for both the SM3 and the SMX beamlines is the use of a multi-mode Raman microprobe head. This is illustrated in Figure 7 with plans developed in collaboration with Horiba-JY Inc. The multi-mode head will accommodate four laser excitation energies. The critical elements within the multi-mode microprobe head are the use of two pairs of dual notch filters. Importantly, each dual

notch filter is selected as a function of the two laser excitation energies to be used, which will be at least 200 nm apart. Consequently, the microprobe head is appropriate for use with 785nm, 633nm, 532nm, and 473/440nm excitation. Thus, a single multi-mode microprobe head will support non-resonant and resonance Raman analysis. This will be of use great benefit to a wide range of researchers (see Table 1 and letters in Appendix III). Moreover, with an on-lilne visualization camera, it will be easy to align the microprobe head to the eucentric rotation point of the crystal, the x-ray beam, and the other complementary spectroscopic methods deployed at the beamline.

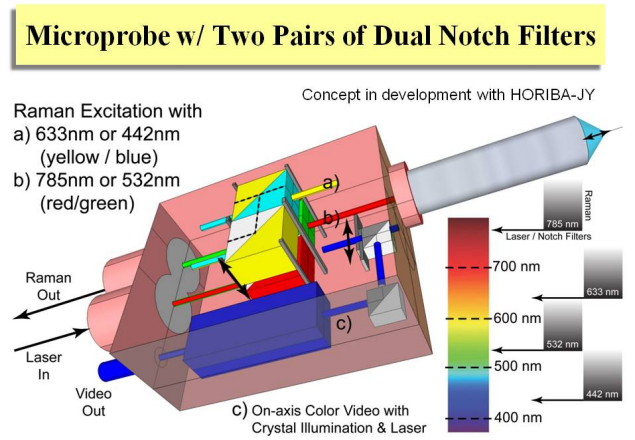

Fig. 7: Raman multi-mode microprobes under development by Horiba-JY for use at SM3 and SMX beamlines.

XAS and x-ray diffraction both utilize detectors that require a relatively large foot-print nearest the sample. Methods that allow these two detector types to come as close as possible without compromising the data quality of either detector type would benefit the nearly simultaneous data collection strategy from these techniques. Motorized stages and full integration of the data collection modes into the beamline control software are relatively simple solutions, but other more creative strategies are also possible. For example, a simple taper to the otherwise box-shape of these detectors will allow a closer approach between them.

D. User Community and Demands

The nine existing MX beamlines at NSLS are an amazing engine for structural biology. In particular, since the beginning of 2005 there have been 2800 PDB submissions and 1795 new publications discovered from the nine active and two legacy* NSLS beamlines: X3-A, X4-A, X4-C, X6-A, X8-C*, X9-A*, X12-B, X12-C, X25, X26-C, and X29. Of the publications, over 10%, 185 were in the premier journals *Science*, *Nature*, and *Cell*. We also observe that X29 is now the second most productive beamline in the world in PDB depositions with 250 in 2009. The highest number is 290 from the BER-funded third-generation undulator 19ID at the APS. No other beamline comes close. Three recent winners in the Nobel Prize in Chemistry, Roderick MacKinnon in 2003, and Venkatraman Ramakrishnan, and Thomas Steitz in 2009, employed beamline X25 and other NSLS beamlines for significant portions of their prize-winning work.

The combination of high resolution x-ray diffraction with UV/vis and vibrational spectroscopies is currently providing valuable information relevant to reaction mechanisms and radiation effects (*3, 6, 7, 16-18*). Similar facilities are either in operation or under construction at nearly every synchrotron world-wide (*12, 19-21*). Beamline X26-C of the National Synchrotron Light Source (NSLS) is the only facility in the United States to offer the user community the ability to collect correlated measurements of up to three types of complementary data -- x-ray diffraction to high resolution, optical absorption spectroscopy, and Raman spectroscopy -- from the same sample and under nearly identical experimental conditions. **Our current user community will demand continuity of this critical capability when NSLS transitions to NSLS-II.**

The single-crystal spectroscopy facility and data collection strategies we are developing now at beamline X26-C of the NSLS will enable us to establish similar, but *more comprehensive* facilities at the NSLS-II. Many research groups are very interested in exploiting the capabilities anticipated at the SMX and SM3 beamlines (please see supporting letters). Indeed, some of these groups are currently using beamline X26-C. For example, Dr. Zhou and coworkers of Columbia University are developing an atomic level understanding of the K^+ ion channel transporter, TrkG, which is regulated by intracellular NADH. At another extreme, Dr. Kerfeld and coworkers of the Joint Genome Institute and the University of California, Berkeley are studying the orange carotenoid protein (OCP) from cyanobacteria. This photon-sensing and signaling protein helps cyanobacteria defend against reactive oxygen species generated by intense sunlight.

Selected References:

1. NIH. (2008) New Pathways to Discovery, in *NIH Roadmap Initiatives*, Office of Portfolio Analysis and Strategic Initiatives, Bethesda, Maryland.
2. Waldron, K. J., Rutherford, J. C., Ford, D., and Robinson, N. J. (2009) Metalloproteins and metal sensing, *Nature 460*, 823-830.
3. Berglund, G. I., Carlsson, G. H., Smith, A. T., Szoke, H., Henriksen, A., and Hajdu, J. (2002) The catalytic pathway of horseradish peroxidase at high resolution, *Nature 417*, 463-468.
4. Katona, G., Carpentier, P., Niviere, V., Amara, P., Adam, V., Ohana, J., Tsanov, N., and Bourgeois, D. (2007) Raman-assisted crystallography reveals end-on peroxide intermediates in a nonheme iron enzyme, *Science (New York, N.Y 316*, 449-453.
5. Hersleth, H. P., Uchida, T., Rohr, A. K., Teschner, T., Schunemann, V., Kitagawa, T., Trautwein, A. X., Gorbitz, C. H., and Andersson, K. K. (2007) Crystallographic and Spectroscopic Studies of Peroxide-derived Myoglobin Compound II and Occurrence of Protonated Fe^{IV}-O^{-}, *J Biol Chem 282*, 23372-23386.
6. Meharenna, Y. T., Doukov, T., Li, H., Soltis, S. M., and Poulos, T. L. (2010) Crystallographic and single-crystal spectral analysis of the peroxidase ferryl intermediate, *Biochemistry 49*, 2984-2986.
7. Orville, A. M., Lountos, G. T., Finnegan, S., Gadda, G., and Prabhakar, R. (2009) Crystallographic, spectroscopic, and computational analysis of a flavin C4a-oxygen adduct in choline oxidase, *Biochemistry 48*, 720-728.
8. Royant, A., Carpentier, P., Ohana, J., McGeehan, J., Paetzold, B., Noirclerc-Savoye, M., Vernede, X., Adam, V., and Bourgeois, D. (2007) Advances in spectroscopic methods for biological crystals. 1. Fluorescence lifetime measurements, *J Appl Crystallog 40*, 1105-1112.
9. Valley, M. P., Tichy, S. E., and Fitzpatrick, P. F. (2005) Establishing the kinetic competency of the cationic imine intermediate in nitroalkane oxidase, *J Am Chem Soc 127*, 2062-2066.
10. Gadda, G., and Fitzpatrick, P. F. (1998) Biochemical and physical characterization of the active FAD-containing form of nitroalkane oxidase from *Fusarium oxysporum*, *Biochemistry 37*, 6154-6164.
11. Pushkar, Y., Yano, J., Sauer, K., Boussac, A., and Yachandra, V. K. (2008) Structural changes in the Mn_4Ca cluster and the mechanism of photosynthetic water splitting, *Proceedings of the National Academy of Sciences of the United States of America 105*, 1879-1884.
12. Ellis, M. J., Buffey, S. G., Hough, M. A., and Hasnain, S. S. (2008) On-line optical and x-ray spectroscopies with crystallography: an integrated approach for determining metalloprotein structures in functionally well defined states, *J Synch Rad 15*, 433-439.
13. Yano, J., Kern, J., Sauer, K., Latimer, M. J., Pushkar, Y., Biesiadka, J., Loll, B., Saenger, W., Messinger, J., Zouni, A., and Yachandra, V. K. (2006) Where water is oxidized to dioxygen: structure of the photosynthetic Mn4Ca cluster, *Science 314*, 821-825.
14. Yano, J., Kern, J., Irrgang, K. D., Latimer, M. J., Bergmann, U., Glatzel, P., Pushkar, Y., Biesiadka, J., Loll, B., Sauer, K., Messinger, J., Zouni, A., and Yachandra, V. K. (2005) X-ray damage to the Mn4Ca complex in single crystals of photosystem II: a case study for metalloprotein crystallography, *Proceedings of the National Academy of Sciences of the United States of America 102*, 12047-12052.
15. Latimer, M. J., Ito, K., McPhillips, S. E., and Hedman, B. (2005) Integrated instrumentation for combined polarized single-crystal XAS and diffraction data acquisition for biological applications, *J Synch Rad 12*, 23-27.
16. Héroux, A., Bozinovski, D. M., Valley, M. P., Fitzpatrick, P. F., and Orville, A. M. (2009) Crystal structures of intermediates in the nitroalkane oxidase reaction, *Biochemistry 48*, 3407-3416.
17. Jensen, L. M., Sanishvili, R., Davidson, V. L., and Wilmot, C. M. (2010) In crystallo posttranslational modification within a MauG/pre-methylamine dehydrogenase complex, *Science 327*, 1392-1394.
18. Wilmot, C. M., and Davidson, V. L. (2009) Uncovering novel biochemistry in the mechanism of tryptophan tryptophylquinone cofactor biosynthesis, *Current opinion in chemical biology 13*, 469-474.
19. Davies, R. J., Burghammer, M., and Riekel, C. (2009) A combined microRaman and microdiffraction set-up at the European Synchrotron Radiation Facility ID13 beamline, *J Synch Rad 16*, 22-29.
20. McGeehan, J., Ravelli, R. B., Murray, J. W., Owen, R. L., Cipriani, F., McSweeney, S., Weik, M., and Garman, E. F. (2009) Colouring cryo-cooled crystals: online microspectrophotometry, *J Synch Rad 16*, 163-172.
21. Owen, R. L., Pearson, A. R., Meents, A., Boehler, P., Thominet, V., and Schulze-Briese, C. (2009) A new on-axis multimode spectrometer for the macromolecular crystallography beamlines of the Swiss Light Source, *J Synch Rad 16*, 173-182.